

We are IntechOpen, the world's leading publisher of Open Access books Built by scientists, for scientists

6,900

Open access books available

186,000

International authors and editors

200M

Downloads

Our authors are among the

154

Countries delivered to

TOP 1%

most cited scientists

12.2%

Contributors from top 500 universities



WEB OF SCIENCE™

Selection of our books indexed in the Book Citation Index
in Web of Science™ Core Collection (BKCI)

Interested in publishing with us?
Contact book.department@intechopen.com

Numbers displayed above are based on latest data collected.
For more information visit www.intechopen.com



Multilayer Fresnel Zone Plate with High-Diffraction Efficiency: Application of Composite Layer to X-ray Optics

Shigeharu Tamura




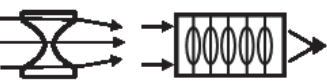


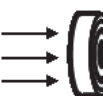
*National Institute of Advanced Science and Technology (AIST), Osaka
Japan*

1. Introduction

Composite materials are widely utilized in a number of fields, such as materials science, metallurgy, polymer science, interface science, mechanical engineering and aerospace engineering. In this chapter, as an application of a composite material layer (thin film) produced by co-sputtering to the hard X-ray focusing optical technique, a multilayer Fresnel zone plate (ML-FZP) with high diffraction efficiency is described. X-rays in the energy region of 100 – 2,000 eV (2 keV) are called soft X-rays (Snigirev & Snigireva, 2008), while those with higher energy are called hard X-rays. Soft X-rays, especially in the “water window” region (Spiller, 1994), are mainly used in the field of biotechnology. On the other hand, hard X-rays are used in various research fields, including materials science, environmental science and medical science.

High brilliant hard X-ray beams with submicron- or nanometre-scale spot sizes generated by third-generation synchrotron radiation (SR) facilities such as the APS (USA), ESRF (France) or SPring-8 (Japan), especially for use in the high-energy region, have great potential for use in various fields of research. They are remarkably powerful tools. Recently, higher energy (shorter wavelength) X-ray beams above 20 keV have been utilised in a number of applications, including residual stress measurement in metal matrix composites at 40 keV (Korsunsky & Wells, 2000), local strain measurement within bulk materials at 52 and 90 keV (Lienert et al., 2000), a novel experimental scheme for high-resolution X-ray analysis of deeply buried interfaces at 71.3 keV (Reichert et al., 2003), study of the ice-SiO₂ model interface, using X-ray transmission-reflection scheme at 71.3 keV (Engemann et al., 2004), mapping of Sr in (Ba,Sr)TiO₃ dielectric ceramics using *K α* fluorescence X-rays at 25 keV (Takeuchi et al., 2005), micro-XRF (X-ray fluorescence) analysis of heavy metals in the cells of hyperaccumulator plants at 37 and 75 keV (Terada et al., 2004; Terada et al., 2005), non-destructive imaging of integrated circuits (ICs) at 25 keV, and imaging of Au mesh by three types of X-ray microscopy at 82 keV (Awaji et al., 2003; Suzuki et al., 2006). In addition, microscopic imaging of Au mesh at 200 keV has also been reported (Kamijo et al., 2009).

Many types of focusing optics have been developed for hard X-rays and their focusing abilities have been improved over the past two decades. Especially within the last several years, there have been dramatic changes in the performances of focusing optics. The main types of focusing optics and their performances are shown in Fig. 1.

Focusing Optics	1988 ~ around year 2000	year 2005 ~
(a)  Bragg-Fresnel lens	⊙ $0.7 \times 0.7 \text{ }\mu\text{m}$ (7.6 keV) [1]	
(b)  Wolter mirror	⊙ $1.6 \times 34 \text{ }\mu\text{m}$ (8 keV) [2]	
(c)  K-B mirror (Kirkpatrick-Baez)	⊙ $5 \times 5 \text{ }\mu\text{m}$ (10 keV) [3]	● 7 nm (20 keV) [4] ⊙ $30 \times 50 \text{ nm}$ (15 keV) [5] ⊙ $0.35 \times 0.4 \text{ }\mu\text{m}$ (80 keV) [6] ⊙ $0.9 \times 1.2 \text{ }\mu\text{m}$ (100 keV) [7]
(d)  Refractive lens	● $8 \text{ }\mu\text{m}$ [linear] (14 keV) [8] ◆ $0.4 \text{ }\mu\text{m}$ (23.5 keV) [9]	⊙ $1.5 \times 3.1 \text{ }\mu\text{m}$ (78 keV) [10] ● $5 \sim 10 \text{ }\mu\text{m}$ (212 keV) [10, 11] ⊙ $47 \times 55 \text{ nm}$ (21 keV) [12, 13]
(e)  Multilayer Laue lens		● 16 nm (19.5 keV) [14] ● 13 nm (20 keV) [15] ◆ 50 nm (20 keV) [16]
(f)  Fresnel zone Plate (FZP)	⊙ $0.6 \times 0.7 \text{ }\mu\text{m}$ (8 keV) [17] ⊙ $7 \times 9 \text{ }\mu\text{m}$ (50 keV) by 2-FZP [18] ▲ 55 % (7 keV) [19, 20]	◆ 40 nm (8 keV) [21] ⊙ 58 nm (8 keV) [22] ⊙ 35 nm (8 keV) [23]
(g)  Multilayer FZP (ML-FZP)	⊙ $3 \times 10 \text{ }\mu\text{m}$ (8 keV) [24, 25] ⊙ $0.5 \text{ }\mu\text{m}$ (8 keV) [26, 27] ◆ 100 nm (12.4 keV, 15 keV) [28, 29]	⊙ $0.5 \text{ }\mu\text{m}$ (100 keV) [30] ⊙ $0.6 \times 20 \text{ }\mu\text{m}$ (200 keV) [31] ▲ 50 % (50 keV) [32] ▲ 52 % (70 keV) [33]

⊙ beam size (2D) , ● beam size (1D) , ◆ spatial resolution (2D), ▲ diffraction efficiency

Fig. 1. Various focusing optics for synchrotron radiation (SR) X-ray.

Representative results (measured numerical datum) in Fig.1 are as follows: [1] (Snigirev et al., 1995), [2] (Hayakawa et al., 1989), [3] (Underwood et al., 1988), [4] (Mimura et al., 2010), [5] (Matsuyama et al.; 2006), [6-7] (Suzuki et al.; 2007), [8] (Snigirev et al., 1996), [9] (Lengeler et al., 1999), [10] (Snigirev et al., 2004), [11] (Nazmov et al, 2005), [12] (Schroer et al., 2006), [13] (Schroer et al., 2005), [14] (Kang et al., 2008), [15] (Koyama et al., 2010a), [16] (Koyama et al., 2010b), [17] (Lai et al., 1992), [18] (Shastri et al., 2001), [19] (Fabrizio et al., 1999a), [20] (Fabrizio et al., 1999b), [21] (Chu et al., 2008), [22] (Suzuki et al., 2005), [23] (Suzuki et al., 2010), [24] (Saitoh et al., 1988), [25] (Saitoh et al., 1989), [26] (Kamijo et al., 1997), [27] (Suzuki et al., 1997), [28] (Kamijo et al., 2002a), [29] (Kamijo et al., 2002b), [30] (Kamijo et al., 2003), [31] (Kamijo et al., 2009), [32] (Tamura et al., 2006), [33] (Tamura et al., 2008). At present, only the ML-FZP, K-B mirror and Refractive lens have achieved focusing above an X-ray energy of 100 keV. Recently, new types of optics have been proposed (Takano et al., 2010; Suzuki et al., 2010a). Among the optics shown in Fig. 1, FZP has advantages in that the optical system can be constructed easily (the tilting angle of the FZP is easily adjustable to the optical axis). In addition, ML-FZP has the important advantages that the kinoform type (theoretical diffraction efficiency, 100%) (Erko et al., 1996) can be fabricated, and that it can operate in the high-energy X-ray region (> 100 keV) because a large “aspect ratio” structure can be realised relatively easily. The most important characteristics of the FZP are its high diffraction efficiency, high spatial resolution and availability in the high-energy X-ray

region. Here, the author describes (1) the process of fabrication and testing of the ML-FZP and (2) the development of ML-FZP with high diffraction efficiency using composite thin film layers.

2. Fresnel zone plate (FZP)

The normal FZP is a circular diffraction grating of alternate transparent and opaque zones. The outline of the FZP is shown in Fig. 2 (details of the schematics of various types of the FZP are shown in Fig. 6). The FZPs have mainly been fabricated by a lithography-based technique or by a sputtered-sliced one (ML-FZP). As mentioned above, the ML-FZP has many advantages. The zone width decreases gradually from the centre to the outer edge.

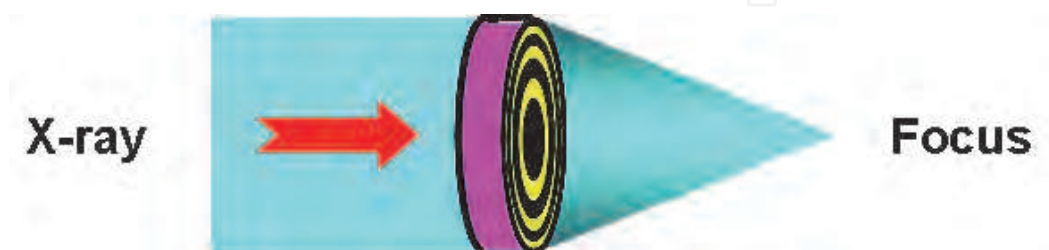


Fig. 2. Schematic of Fresnel zone plates

The radius r_n of the n th zone is given by

$$r_n^2 = r_0^2 + n\lambda f \quad (1)$$

where r_0 is the radius of the central zone (wire substrate), λ is the X-ray wavelength and f is the focal length. The spatial resolution D of the FZP for the first-order focus is determined by the outermost (minimum) zone width dr

$$D = 1.22 \, dr \quad (2)$$

The focal spot size is comparable to the spatial resolution. The theoretical diffraction efficiency of the normal type (an amplitude modulation) FZP is 10 %. The efficiencies of the phase modulating type FZP are described elsewhere (Kirz, 1974; Yun et al., 1992; Bionta et al., 1994; Tamura et al., 2000; Kamijo et al., 2000).

3. Fabrication of normal multilayer Fresnel zone plate (ML-FZP)

3.1 Deposition of multilayer

The ML-FZP is or often called a “sputtered-sliced” zone plate. The conventional-type ML-FZP is composed of multiple concentric layers of alternating high-Z (*i.e.*, large atomic number) and low-Z (*i.e.*, small atomic number) materials. Hart et al. (Hart et al., 1966) and Rudolph et al. (Rudolph et al., 1981) proposed the concept of the ML-FZP. WSi_2/C FZP and Cu/Al FZP were subsequently developed and tested by Saitoh et al. (Saitoh et al., 1988; Saitoh et al., 1989) and Bionta *et al.* (Bionta et al., 1989; Bionta et al. 1990), respectively. However, these experiments did not achieve focusing with submicron spot size. Figure 3 presents an outline of the fabrication process of ML-FZP (normal type), which consisted of two parts: deposition and mechanical manufacturing. As a preliminary experiment, various concentric multilayer samples (W/C , Cr/C , Ag/C , Cu/C , Cu/Al , NiCr/Al , *etc.*) were fabricated and the roughness

of their multilayer interfaces (zone) was examined. Among these samples, the Cu/Al multilayer formed comparatively smooth zones and a polished surface (Tamura et al., 1994). Therefore, the Cu/Al multilayer coating is described in this chapter.

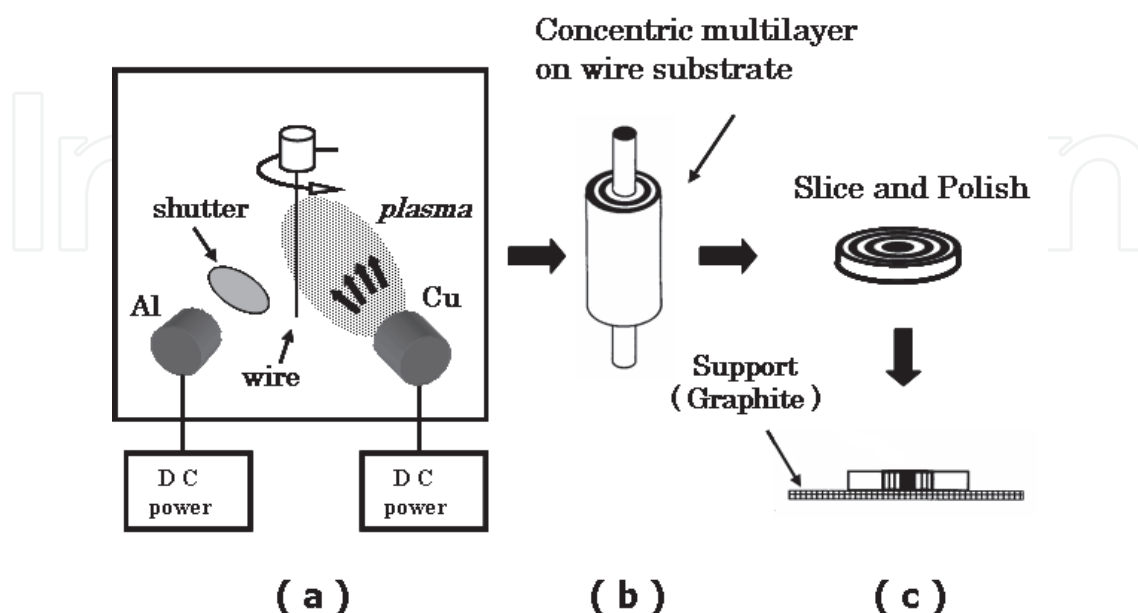


Fig. 3. Fabrication of multilayer Fresnel zone plate (ML-FZP): (a) schematic diagram of DC sputtering apparatus, (b) deposited sample, and (c) fabrication of FZP.

The Cu/Al concentric multilayer samples were deposited onto a rotating (15 – 50 rpm) Au wire substrate 50 micron in diameter by a DC magnetron sputtering apparatus with two DC-sputtering guns (3 inches in diameter) placed at the base points of a right triangle with the Au wire at the apex. The gun-to-substrate distance was 50 mm. The layer thickness was monitored and controlled by a quartz thickness monitor. To achieve smooth zones, if necessary, a cylindrical slit (linear slit fabricated on the surface of a stainless cylindrical shield) was used between the target and the substrate in the sputtering apparatus (Yasumoto et al., 2001; Tamura et al., 2002). The slit was controlled automatically such that it faced the operating sputtering gun. Figure 4 shows photographs of the sputtering apparatus. The Cu/Al samples were fabricated under conditions with various deposition parameters. Representative deposition parameters were as follows: sputtering power, 6 W cm⁻² for Cu and 10 W cm⁻² for Al; total gas pressure, 0.2 Pa; and coating rate, 0.3 nm s⁻¹ for both Cu and Al layers. A protective overcoat layer (Cu, 3 micron) was also deposited.

3.2 Fabrication of zone plate

After the deposition process, the multilayer wire sample was embedded into low melting point alloy (melting point: 453 K), sliced into a plate 1 mm thick perpendicular to the wire axis using a band saw micro-cutting machine. One sliced surface was polished mechanically using a micro-grinding machine (wet process) and the layer structure was examined. Next, this polished surface was fixed onto a graphite plate with resin glue and polished until the desired thickness was achieved. Photographs of a sliced sample (embedded in alloy), the FZP fixed on the graphite plate and the scanning electron microscopic (SEM) image of an FZP are shown in Fig. 5.

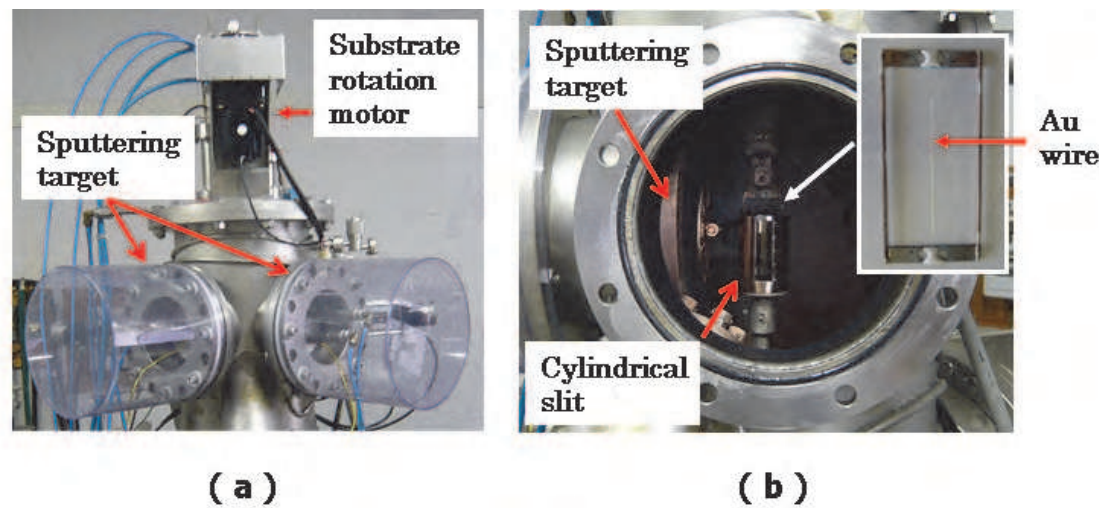


Fig. 4. Photographs of DC sputtering apparatus: (a) sputtering chamber, (b) inside of chamber.

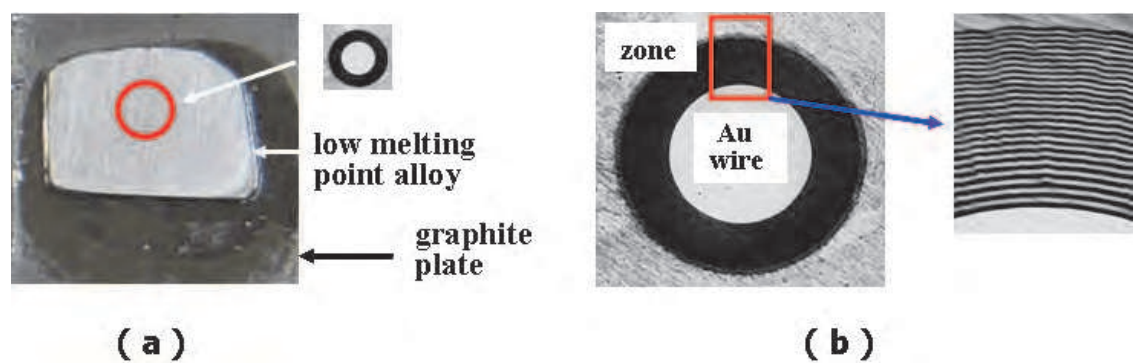


Fig. 5. Multilayer Fresnel zone plate (ML-FZP) : (a) ML-FZP on graphite, (b) Scanning electron micrographs. Black and white zones are Al and Cu layers, respectively.

4. Fabrication of multilevel-type multilayer Fresnel zone plate

4.1 Deposition of multilayer

As mentioned in Section 1, the high diffraction efficiency is one of important performance characteristics of the Fresnel zone plate. The theoretical diffraction efficiency of the normal type (amplitude modulation) FZP is 10% and that of the phase modulating type FZP is 40%. However, the actual efficiencies are 10% – 20%. This reduction in performance is due to fabrication error and absorption by the material. In X-ray microscopy optical systems using the FZP, higher diffraction efficiency is necessary to reduce radiation damage to biological specimens (Fujisaki & Nakagiri, 1990) and to simplify the optical system because this considerably suppresses unwanted diffraction orders (Fabrizio et al., 1999a). Among the various types of FZP, the kinoform FZP has the highest theoretical diffraction efficiency of 100% (Erko et al., 1996), although it is extremely difficult to fabricate such an FZP precisely. A multilevel-type FZP fabricated by the lithography-based technique has been proposed (Fabrizio et al., 1994) and developed as an approximate structure for the kinoform FZP, and it showed efficiency of 55% at 7 keV (Fabrizio et al., 1999a; Fabrizio et al., 1999b). Such an FZP, however, cannot function in the high-energy region (above 20 keV) because it is

technically difficult to realise a high aspect ratio (*i.e.*, the ratio of FZP thickness to the zone width). Schematic representations of various types of FZP are shown in Fig. 6.

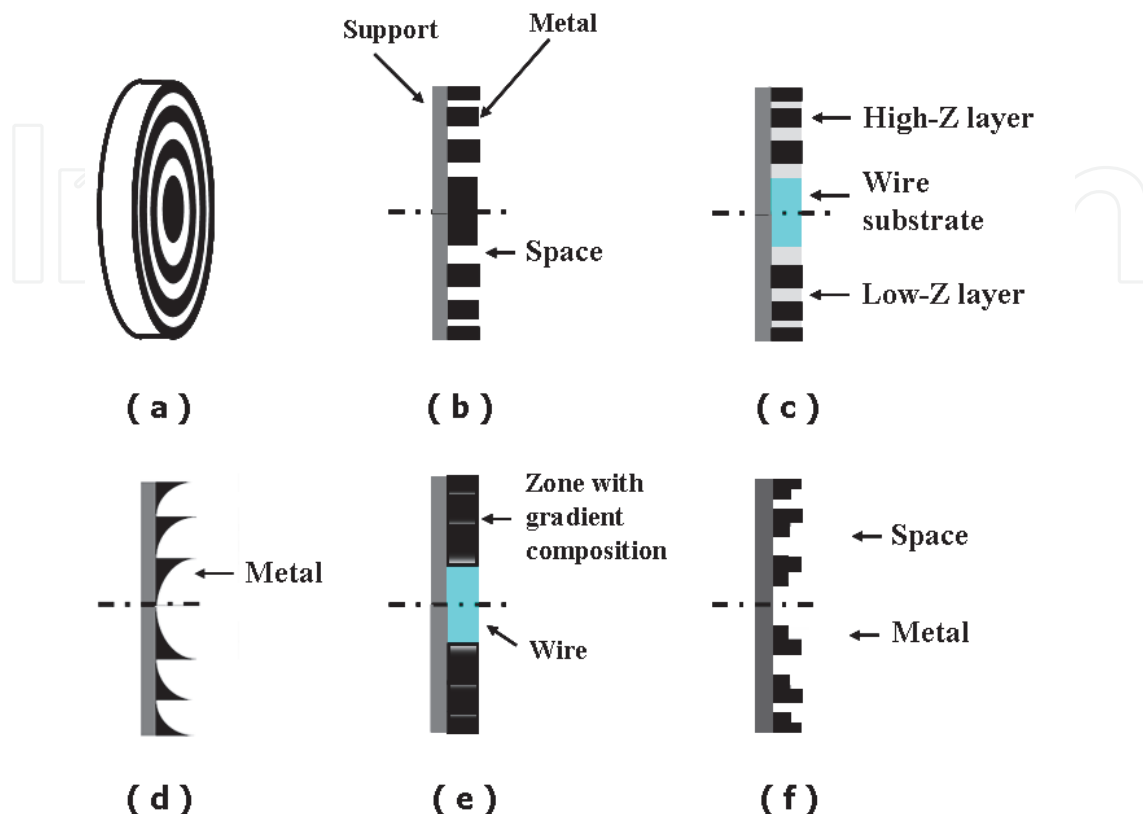


Fig. 6. Schematics of Fresnel zone plates (FZP): (a) schematic image, (b) FZP by lithography-based technique, (c) FZP by sputtered-sliced technique, (d) kinoform zone plate by lithography-based technique, (e) kinoform sputtered-sliced zone plate, and (f) 3-step multilevel zone plate by lithography-based technique.

4.2 Fabrication of zone plate

Schematic representations of the 1-period structure of various FZPs are shown in Fig. 7. As a preliminary experiment, a multilevel-type ML-FZP (5-period, total of 15 layers) with 3-step structure (Fig. 7(e)) was fabricated on the assumption that this ML-FZP composed of high-Z (Cu), low-Z (Al) and composite layers (Cu:Al = 1:1) was functionally equivalent to the FZP with the structure shown in Fig. 7(b). The composite layer was deposited by co-sputtering of high-Z and low-Z materials with the same coating rate. The focusing characteristics were evaluated at SPring-8 by comparing the 1st and -1st order diffraction at a CCD detector located downstream of the focal point. The details of the focusing test are described later. At the normal FZP, the intensity of the 1st order diffraction was the same as that of the -1st order diffraction. On the other hand, at this 3-step ML-FZP, the intensity of the 1st order diffraction was somewhat higher than that of the -1st order diffraction. These observations indicated that this composite layer fabricated by co-sputtering functions well and contributes to the improvement of diffraction efficiency.

Several types of 3-step, 4-step and 6-step ML-FZP were fabricated. As an example, the deposition of the 4-step multilayer is described. The concentric multilayer sample for the multilevel-type FZP was designed according to the theory presented by Fabrizio et al.

(Fabrizio et al., 1994). The designed focal length was 200 mm at 12.4 keV. Such a multilayer is composed of multiple concentric layers of alternating high-Z (Cu), low-Z (Al), and two types of composite material (Cu, Al) layers: zone-1 is a Cu layer, zone-2 is a composite layer (Cu:Al = 2:1), zone-3 is a composite layer (Cu:Al = 1:2) and zone-4 is an Al layer. The composite layers were deposited by co-sputtering of high-Z and low-Z materials, and the composition of the composite layers was controlled by changing the power of each target (*i.e.*, by controlling each coating rate). A total of 60 layers (15 pairs) were deposited. The inner zone (Al) was 0.2 micron in width and the outermost zone (Cu) was 0.15 micron in width. The theoretical focused beam size was 0.61 multiplied by the zone width of the outermost one pair zones (*i.e.*, the amount of 4 kinds of zones). Deposition parameters were as follows: sputtering powers were 2.7 W/cm² for Cu (zone-1), 5 W/cm² for Al (zone-4), 1.8 W/cm² for Cu, and 1.6 W/cm² for Al (zone-2), 0.9 W/cm² for Cu and 3.2 W/cm² for Al (zone-3). Ar gas pressure was 0.2 Pa. The substrate temperature was not controlled, the coating rate was 0.7 nm/s and the thickness of the FZP was 55 micron.

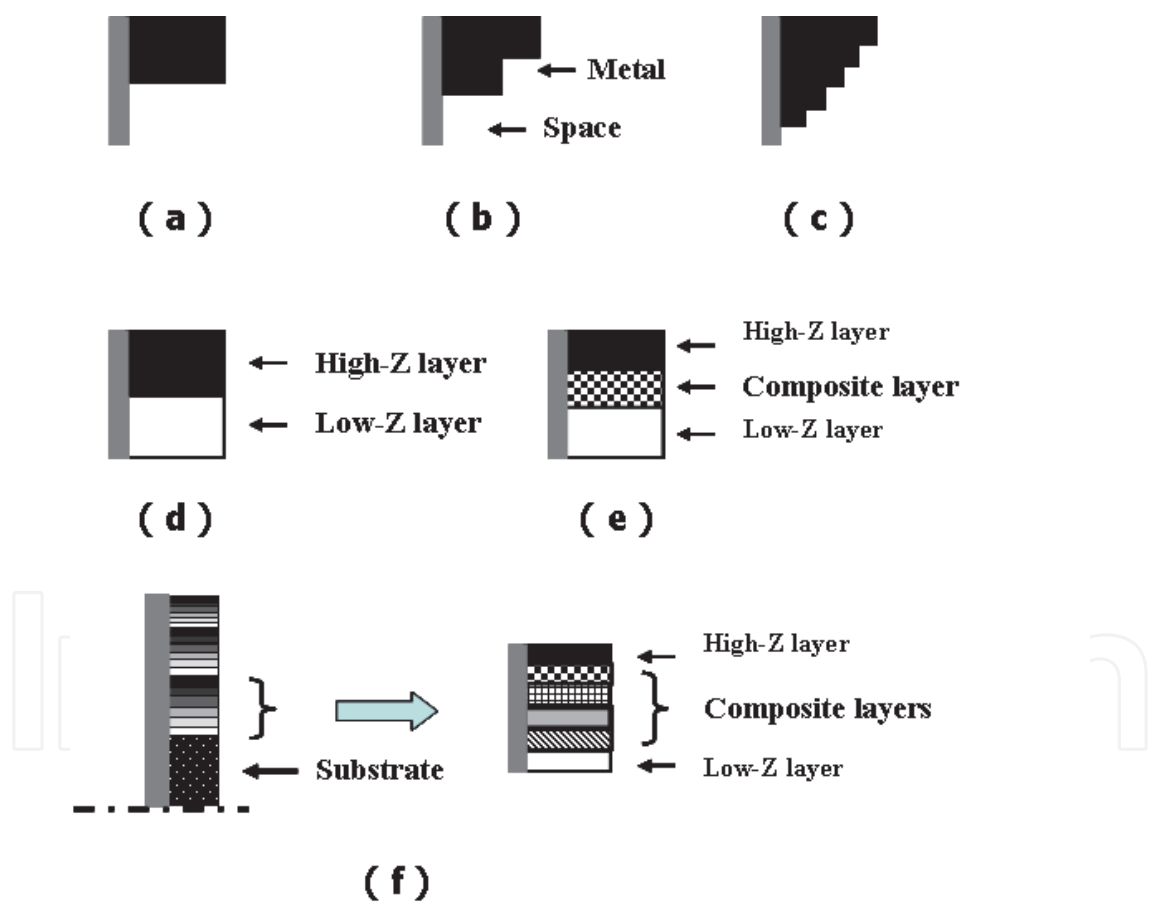


Fig. 7. Schematics of one-period structure of Fresnel zone plates (FZP): (a) conventional FZP by lithography-based technique, (b) 3-step multilevel FZP by lithography-based technique, (c) 6-step multilevel FZP by lithography-based technique, (d) conventional FZP by sputtered-sliced technique, (e) 3-step multilevel FZP by sputtered-sliced technique, and (f) 6-step multilevel FZP by sputtered-sliced technique.

In a similar manner, two 6-step ML-FZPs were fabricated with thicknesses of 35 micron and 66 micron, respectively. SEM images of the 3-step and 6-step ML-FZP are shown in Fig. 8, along with the results of Energy Dispersive X-ray (EDX) line scanning along the multilayer surface. Accurate analysis could not be done because of the resolution of the EDX equipment (0.5 micron). As shown in Fig.8, zone (multilayer interface) roughness towards the top of the layer stack is observed. Such a roughness is caused by the complex structure of the sputtered thin film (Thornton, 1974; Thornton, 1986).

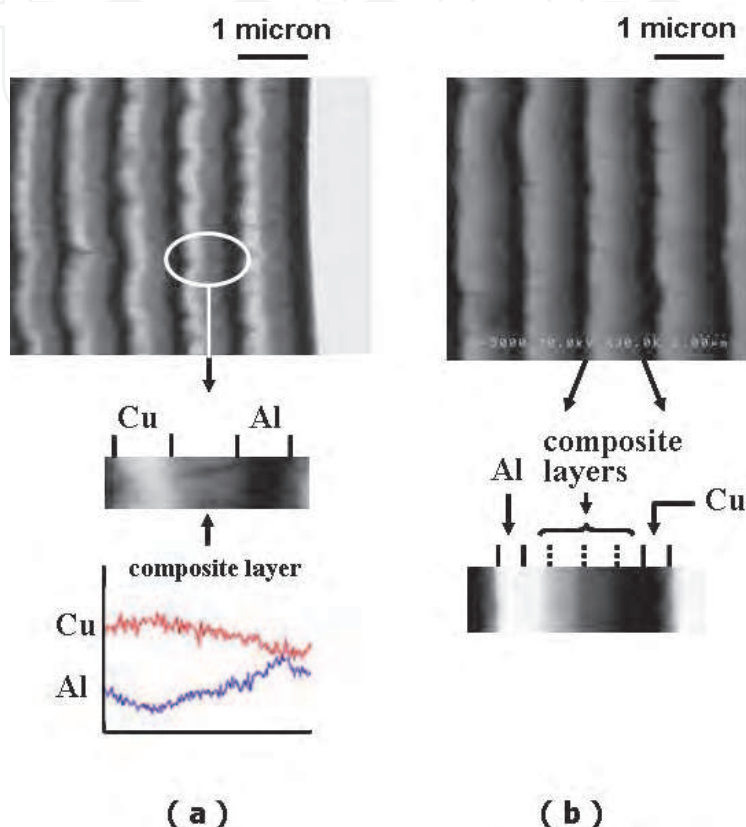


Fig. 8. Scanning electron micrographs (close-up view) of multilevel multilayer FZP: (a) 3-step FZP and its scanning of the energy dispersive X-ray (EDX) along the multilayer surface, and (b) 6-step FZP. Black and white zones are Al and Cu layers, respectively. Another gray zones are composite layers.

5. Focusing test of multilayer Fresnel zone plate

5.1 Focused beam size and spatial resolution

Focusing tests of various ML-FZPs were performed at the BL20XU or BL47XU undulator beamline of SPring-8. A representative experimental setup of the beamline is described previously (Kamijo et al., 2002a; Kamijo et al., 2003; Suzuki et al., 2001). Photographs of the experimental facilities are shown in Fig. 9. The focused beam size, the spatial resolution and the diffraction efficiency were measured as necessary. The focused beam size [full width at half maximum (FWHM)] was measured by conventional knife-edge scan. As shown in Fig. 1, representative results were a spot size of 500 nm at 100 keV and focusing at 200 keV (Kamijo et al., 2003; Kamijo et al., 2009). The spatial resolution was measured by observing an X-ray microscopic image of a resolution test pattern with a tantalum microstructure. The

representative result was 100 nm at 12.4 keV and at 15 keV (Kamijo et al., 2002b; Kamijo et al., 2003).

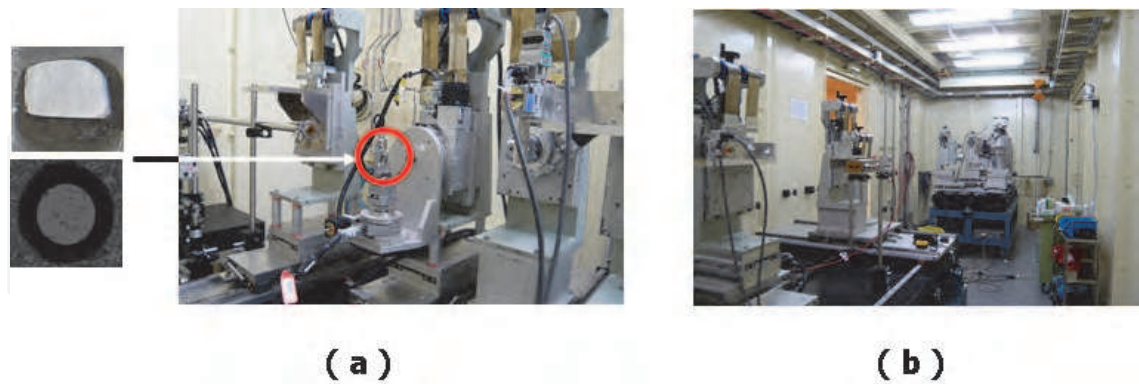


Fig. 9. Photographs of the experimental facilities at Spring-8: (a) facilities around FZP, and (b) facilities in experimental hutch.

5.2 Diffraction efficiency

To examine the effectiveness of the use of the composite layer as shown in Fig. 7, the diffraction efficiencies of three types of ML-FZP discussed above were measured. The diffraction efficiency at the focal point was estimated by comparing the incident beam intensity measured by ion chambers upon the OSA (order sorting aperture: tantalum cross slit) and the total intensity of the focused beam through the OSA (Kamijo et al., 2006). The diffraction efficiency of the 1st order focus and the focused beam size were measured. For the 4-step FZP (thickness 55 micron), the intensity the 1st order diffraction was compared with that of the -1st order diffraction using the refraction corn image at 30 keV. The results indicated that the intensity of the 1st order diffraction was higher than that of the -1st order diffraction (Fig. 10). This FZP was confirmed to function well as an FZP with high diffraction efficiency. The details of this experiment are described were described previously (Kamijo et al., 2006). The diffraction efficiency was next measured in the high energy region and an efficiency of 50% was achieved at 50 keV with a focused beam size of 1 micron.

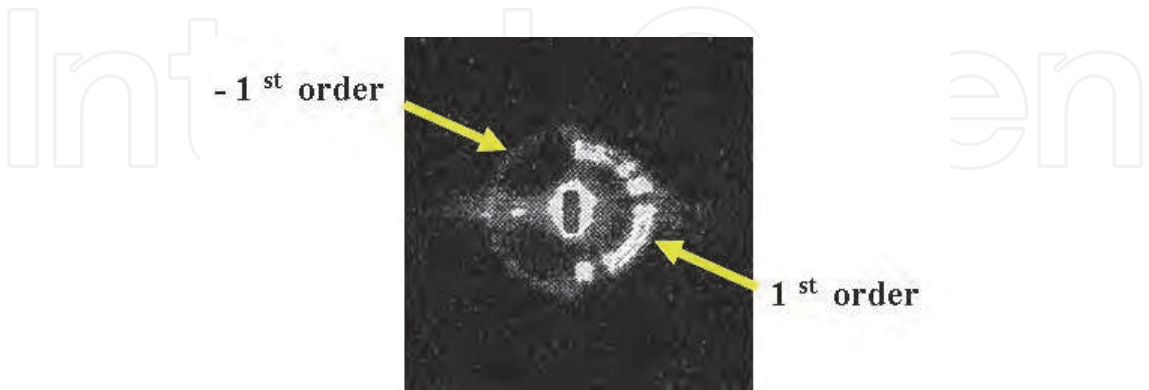


Fig. 10. Refraction corn of 4-step multilayer FZP.

For the 6-step FZP (thickness 35 micron), a 1st order diffraction efficiency of 52% was attained at 41.3 keV with a focused beam size of 0.8 micron. For the 6-step FZP (thickness 66 micron), a 1st order diffraction efficiency of 51% was attained at 70 keV with a focused beam

size of 1.2 micron. The efficiency measured over a wide range is shown in Fig. 11. High diffraction efficiencies over 40%, which is the theoretical limit of the efficiency of the normal FZP, were attained. These experimental results confirmed that the multilevel type ML-FZP using composite layers functioned well like the FZP with a step structure, such as that shown in Fig. 7(c). Despite the zone roughness, these ML-FZPs worked well as X-ray focusing optics.

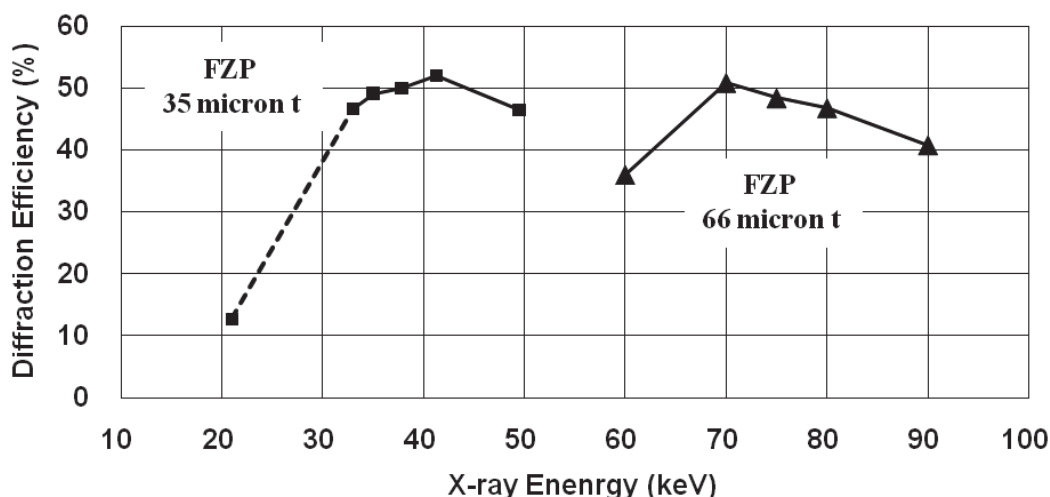


Fig. 11. Measured diffraction efficiencies for 1st-order diffraction for two types of 6-step multilayer FZP.

To achieve high diffraction efficiency in the high-energy X-ray region, multilevel-type multilayer FZPs fabricated with composite layers were developed and tested at the synchrotron radiation beamline at SPring-8. Despite the existence of zone roughness, the experimental results described here confirmed that the proposed multilevel type ML-FZP with composite layers functioned well like the FZP with a step structure fabricated by the lithography-based technique. By precise control of the coating rate in the co-sputtering deposition system, it will be possible to fabricate thin film layers with graded composition structures, which will allow the realisation of kinoform type ML-FZPs with diffraction efficiencies of greater than 80%.

7. X-ray microscopy

As mentioned in Section 1, the ML-FZP is a type of focusing optics for high-energy X-rays at SR facilities. One promising application of the ML-FZP is in X-ray microscopy. Main results of several X-ray microscopy studies using normal ML-FZPs or the 4-step ML-FZP have been reported elsewhere (Takeuchi et al., 2005; Terada et al., 2004; Terada et al., 2005; Kamijo et al., 2003; Suzuki et al., 2001; Kamijo et al., 2006; Takeuchi et al., 2008).

In this section, therefore, other results are shown. Figure 11 presents schematics of representative X-ray microscopy: (a) a scanning microscopy and (b) an imaging microscopy. A scanning X-ray microscopic image of a Au mesh (64 micron pitch) on the PC monitor is shown in Fig.12-(a). This image was taken in the fluorescent mode (detecting Au K-fluorescent X-ray) at 200 keV (Kamijo et al., 2009). A scanning X-ray microscopic image of a Ta test pattern (thickness: 0.5 micron) is shown in Fig.12-(b). This image was taken by using

the 4-step multilevel-type ML-FZP at 23 keV (2nd order light was used without the OSA). The spatial resolution was 500 nm (Kamijo et al., 2006).

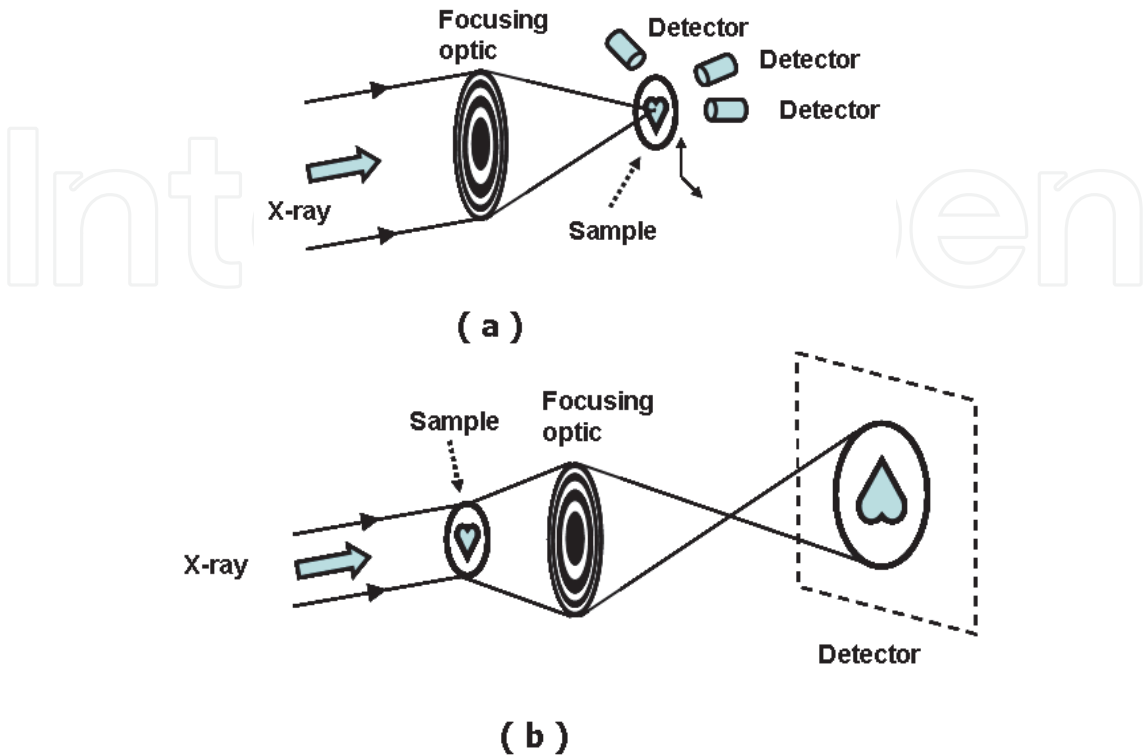


Fig. 11. Schematics of X-ray microscopy: (a) scanning microscopy, (b) imaging microscopy.

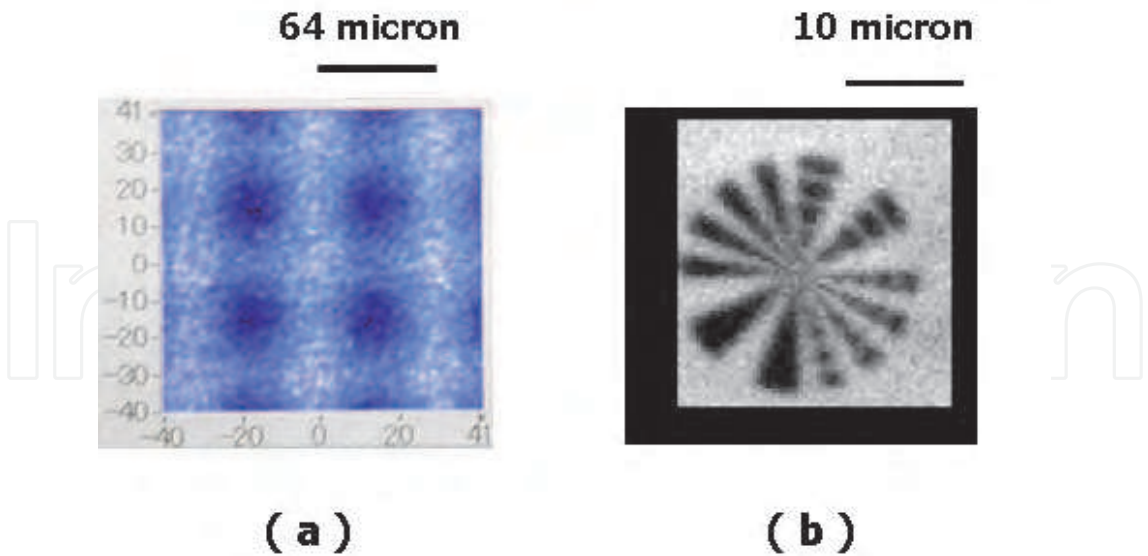


Fig. 12. Scanning X-ray microscopic images by using multilayer Fresnel zone plate: (a) image on PC monitor. (b) transmission x-ray image of Ta test pattern with 0.125 micron step, 0.2 s/pixel.

A scanning microscopic image of a GaAs FET (Gallium Arsenide Field-Effect Transistor) at 27.8 keV is shown in Fig.13 (Tamura et al., 2009).

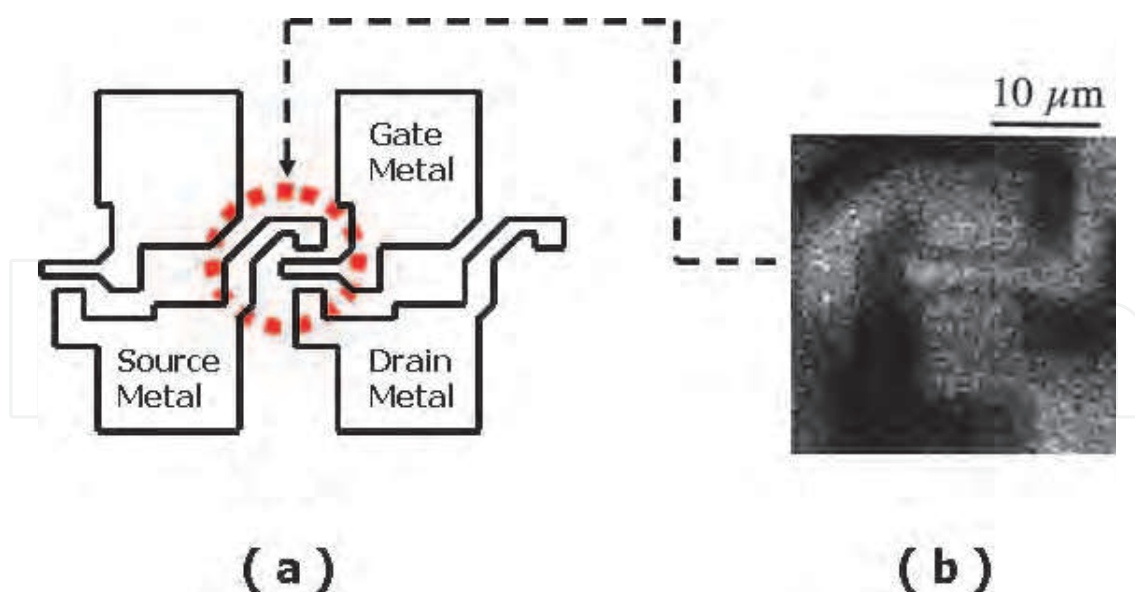


Fig. 13. Scanning X-ray microscopic image of Gallium Arsenide Field-Effect Transistor (GaAs FET) by using multilayer Fresnel zone plate: (a) schematic of GaAs FET, (b) Scanning X-ray microscopic image. Au L-fluorescent X-ray are measured.

8. Conclusions

To achieve high diffraction efficiency in the high-energy X-ray region, multilevel-type multilayer FZPs fabricated with composite layers were developed and tested at the synchrotron radiation beamline at SPring-8. Despite the existence of zone roughness, the experimental results described here confirmed that the proposed multilevel type ML-FZP with composite layers functioned well like the FZP with a step structure fabricated by the lithography-based technique. By precise control of the coating rate in the co-sputtering deposition system, it will be possible to fabricate thin film layers with graded composition structures, which will allow the realisation of kinoform type ML-FZPs with diffraction efficiencies of greater than 80%.

Recently, the microscopic imaging of uranium (L-fluorescent X-ray) by using the K-B mirror as the focusing optics is reported (Terada et al., 2010). Some detail articles have been published concerning X-ray microscopy (Howells et al., 2006) or X-ray focusing optics (Snigirev et al., 2008). Great advance, therefore, will be expected in the field of X-ray microscopy in the near future. In addition, the ML-FZP including multilevel type ML-FZP will be also powerful tools in the field of the hard x-ray three-dimensional microtomography (Takeuchi et al., 2002; Toda et al., 2006).

9. Acknowledgment

The research described in this chapter was performed as collaborative research with SPring-8 (Japan Synchrotron Radiation Research Institute: JASRI). Thanks are due to long-time collaborators Dr. Yoshio Suzuki (SPring-8), Dr. Akihisa Takeuchi (SPring-8), Dr. Kentaro Uesugi (SPring-8), Dr. Mitsuhiro Awaji (SPring-8), Dr. Yasuko Terada (SPring-8), Dr. Masato Yasumoto (AIST) and Dr. Nagao Kamijo (SPring-8, Kansai Medical University, retired AIST). The synchrotron radiation experiments have been performed at SPring-8 with the

approval of the Japan Synchrotron Radiation Research Institute (JASRI) (Proposal No.2004B0180-NM-np, 2005B0269, 2006A1153 and 2006B1747).

10. References

- Awaji, M.; Suzuki, Y.; Takeuchi, A.; Takano, H.; Kamijo, N.; Yasumoto, M.; Terada, Y. & Tamura, S. (2003). Microfocusing of 82 keV X-rays with a sputtered-sliced Fresnel zone plate, *Review of Scientific Instruments*, 74, pp.4948-4949, ISSN 0034-6748
- Bionta, R.M.; Ables, E.; Clamp, O.; Edwards, O.D.; Gabriele, P.C.; Makowiecki, D.; Ott, L.L.; Skulina, K.M. & Thomas, N. (1989). 8 keV x-ray zone plates, *Proc. SPIE (The International Society for Optical Engineering)*, 1160, pp.12-18, ISSN 0277-786X
- Bionta, R.M.; Ables, E.; Clamp, O.; Edwards, Gabriele, P.C.; Ott, L.L., Skulina, K.M. & Viada, T. (1990). Tabletop X-Ray Microscope Using 8 keV Zone Plates, *Optical Engineering*, 29, pp.576-580, ISSN: 0091-3286
- Bionta, R.M.; Skulina, K.M. & Weinberg, J. (1994). Hard x-ray sputtered-sliced zone plates, *Apped. Physics Letters*, 64, pp.945-947, ISSN 0003-6951
- Chu, Y.S.; Yi, J.M.; Carlo, F.De.; Shen, Q.; Lee, Wah-Keat.; Wu, H.J.; Wang, C.L.; Wang, J.Y.; Liu, C.J.; Wang, C.H.; Wu, S.R.; Chien, C.C.; Hwu, Y.; Tkachuk, A.; Yun, W.; Feser, M.; Liang, K.S.; Yang, C.S.; Je, J.H. & Margaritondo, G. (2008). Hard x-ray microscopy with Fresnel zone plates reaches 40 nm Rayleigh resolution, *Applied Physics Letters*, 92, 103119, ISSN 0003-6951
- Engemann, S.; Reichert, H.; Dosch, H.; Bilgram, J.; Honkimäki, V. & Snigirev, A. (2004). Interfacial Melting of Ice in Contact with SiO₂, *Physical Review Letters*, 92, 205701, ISSN 0031-9007
- Erko, A.I.; Aristov, V.V. & Vidal, B. (1996). "Diffraction X-ray Optics", Institute of Physics Publishing, Bristol and Philadelphia, pp.36-40, ISBN 0-7503-0359-X
- Fabrizio, E. Di.; Gentili, M.; Grella, L.; Baciocchi, M.; Krasnoperova, A.; Cerrina, F.; Yun, W.; Lai, B. and Gluskin, E. (1994). High-performance multilevel blazed x-ray microscopy Fresnel zone plates: Fabricated using x-ray lithography, *Journal of Vacuum Science and Technology B*, 12, pp.3979-3985, ISSN 0734-211X
- Fabrizio, E.Di.; Romannato, F.; Gentili, M.; Cabrini, S.; Kaulich, B.; Susini, J. & Barrett, B. (1999a). High-efficiency multilevel zone plates for keV X-rays, *Nature*, 401, pp.895-898, ISSN 0028-0836
- Fabrizio, E.Di. & M.Gentili, M. (1999b). X-ray multilevel zone plate fabrication by means of electron-beam lithography: Toward high-efficiency performances, *Journal of Vacuum Science and Technology B*, 17, pp.3439-3443, ISSN 0734-211X
- Fujisaki, H. & Nakagiri, N. (1990). Design of a gradient refractive index phase zone plate for soft x-rays, *Applied Optics*, 29, pp.483-488, ISSN 0003-6935
- Hart, H.E.; Scrandis, J.B.; Mark, R. & Hatcher, R.D. (1966). Diffraction Characteristics of a Linear Zone Plate, *Journal of the Optical Society of America*, 56, pp.1018-1023, ISSN 0030-3941
- Hayakawa, S.; Iida, A.; Aoki, S. & Gohshi, Y. (1989). Development of a scanning x-ray microprobe with synchrotron radiation, *Review of Scientific Instruments*, 60, pp.2452-2455, ISSN 0034-6748
- Howelles, M.; Jacobsen, C. And Warwick, T. (2006). Principles and Applications of Zone Plate X-Ray Microscopes, *Science of Microscopy (Springer-Verlag)*, pp.835-926, ISBN-10: 0387252967

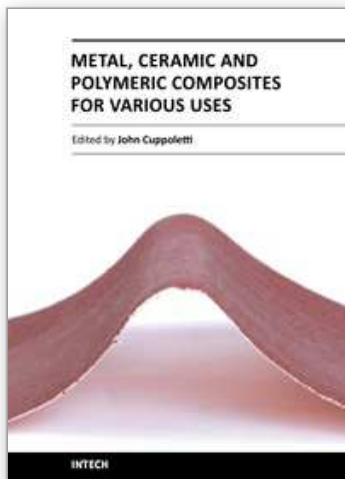
- Kamijo, N.; Suzuki, Y.; Tamura, S.; Handa, K.; Takeuchi, A.; Yamamoto, S.; Ando, M.; Ohsumi, K. & Kihara, H. (1997). Fabrication of Hard X-ray Sputtered-Sliced Fresnel Phase Zone Plate, *Review of Scientific Instruments*, 68, pp.14-16, ISSN 0034-6748
- Kamijo, N.; Suzuki, Y.; Tamura, S.; Awaji, M.; Yasumoto, M.; Kohmura, Y.; Handa, K. & Takeuchi, A. (2000). Fabrication of high energy X-ray Fresnel phase zone plate, *X-Ray Microscopy (Proceedings of the Sixth International Conference)*, pp.672-675, ISSN 0094-243X.
- Kamijo, N.; Suzuki, Y.; Awaji, M.; Takeuchi, A.; Takano, H.; Ninomiya, T.; Tamura, S. & Yasumoto, M. (2002a). Hard X-ray microbeam experiments with a sputtered-sliced Fresnel zone plate and its applications, *Journal of Synchrotron Radiation*, 9, pp.182-186, ISSN 0909-0495
- Kamijo, N.; Suzuki, Y.; Tamura, S.; Takeuchi, A.; Takano, H.; Yasumoto, M. & Awaji, M. (2002b). High resolution microbeam experiment with sputtered-sliced zone plate (II) at 250 m beam line (BL20XU), *SPring-8 User Experiment Report*, No.9, p.134
- Kamijo, N.; Suzuki, S.; Takano, H.; Tamura, S.; Takeuchi, A.; Yasumoto, M. & Awaji, M. (2003). Microbeam of 100 keV X-ray with a sputtered-sliced Fresnel zone plate, *Review of Scientific Instruments*, 74, pp.5101-5104, ISSN 0034-6748
- Kamijo, N.; Suzuki, Y.; Tamura, S.; Takeuchi, A. & Yasumoto, M. (2006). Practical use of quasi-kinoform zone plate : Towards high-efficiency microbeam for hard /high-energy x-rays, *IPAP Conference Series 7 (Institute of Pure and Applied Physics, Japan)*, pp.97-99, ISBN4-900526-21-5
- Kamijo, N.; Suzuki, Y.; Takeuchi, A.; Itou, M. & Tamura, S. (2009). Microbeam of 200 keV x-ray with a sputtered-sliced zone plate, *Japanese journal of Applied Physics*, 48, 010209. ISSN 0021-4922
- Kang, H.C.; Yan, H.; Winarski, R.P.; Holt, M.V.; Maser, J.; Liu, C., Conley, R.; Vogt, S.; Macrander, A.T. & Stephenson, G.B. (2008). Focusing of hard x-rays to 16 nanometers with a multilayer Laue Lens, *Applied Physics Letters*, 92, 221114, ISSN 0003-6951
- Kirz, J. (1974). Phase zone plates for x rays and the extreme uv, *Journal of the Optical Society of America*, 64, pp.301-308, ISSN 0030-3941
- Korsunsky, A.M. & Wells, K.E. (2000). High Energy Synchrotron X-Ray Measurements of 2D Residual Stress States in Metal Matrix Composites, *Materials Science Forum*, 321-324, p.218, ISSN 1662-9752
- Koyama, T.; Takenaka, H.; Ichimaru, S.; Ohchi, T.; Tsuji, T.; Takano, H. & Kagoshima, Y. (2010a). Development of Multilayer Laue Lenses --- (1) Linear Type ---, *Abstract of 10th International Conference on X-ray Microscopy*, P.39
- Koyama, T.; T.; Tsuji, Takano, H.; & Kagoshima, Y.; Ichimaru, S.; Ohchi, T. & Takenaka, H. (2010b). Development of Multilayer Laue Lenses --- (2) Circular Type ---, *Abstract of 10th International Conference on X-ray Microscopy*, P.135
- Lai, B.; Yun, W. B.; Legnini, D.; Xiao, Y.; Crzas, J.; Viccaro, P.J.; White, V.; Denton, D.; Cerrina, F.; Fabrizio, E.; Di; Grella, L. & Baciocchi, M. (1992). Hard x-ray phase zone plate fabricated by lithographic techniques, *Applied Physics Letters*, 61, pp.1877-1879, ISSN 0003-6951

- Lengeler, B.; Schroer, C. G.; Richwin, M.; Tümmler, J.; Drakopoulos, M.; Snigirev, A. & Snigireva, I. (1999). A microscope for hard x-rays based on parabolic compound refractive lenses, *Applied Physics Letters*, 74, pp.3924-3926, ISSN 0003-6951
- Lienert, U.; Poulsen, H.F.; Martins, R.V. & Kwick, A. (2000). A High Energy Microscope for Local Strain Measurements Within Bulk Materials, *Materials Science Forum*, 347-349, P.95, ISSN 1662-9752
- Matsuyama, S.; Mimura, H.; Yumoto, H.; Sano, Y.; Yamamura, K.; Yabashi, M.; Nishino, Y.; Tamasaku, K.; Ishikawa, T. & Yamauchi, K. (2006). Development of scanning X-ray fluorescence microscope with spatial resolution of 30nm using K-B mirrors optics, *Review of Scientific Instruments*, 77, 103102, ISSN 0034-6748
- Mimura, H.; Handa, S.; Kimura, T.; Yumoto, H.; Yamakawa, D.; Yokoyama, H.; Matsuyama, S.; Inagaki, K.; Yamamura, K.; Sano, Y.; Tamasaku, K.; Nishino, Y.; Yabashi, M.; Ishikawa, T. & Yamauchi, K. (2010). Breaking the 10 nanometer barrier in hard X-ray focusing, *Nature Physics*, 6, pp.122-125, ISSN 1745-2473
- Nazmov, V.; Reznikova, E.; Snigirev, A.; Snigireva, I.; DiMichiel, M.; Grigoriev, M.; Mohr, J.; Matthis, B. & V. Saile, V. (2005). LIGA fabrication of X-ray Nickel lenses *Microsystem Technologies*, 11, pp.292-297. ISSN 0946-7076
- Reichert, H.; Honkimäki, V.; Snigirev, A.; Engemann, S. & Dosch, H. (2003). A new Transmission-Reflectivity Scheme using High-Energy X-ray Microbeams for the Study of Deeply buried Interfaces, *Physica*, B336, pp.46-55, ISSN 0921-4526
- Rudolph, D.; Niemann, B. and Schmahl, G. (1981). Status of the Sputtered Sliced Zone Plates For X-Ray Microscopy, *Proc. SPIE (The International Society for Optical Engineering)*, 316, pp.103-105, ISSN 0277-786X
- Saitoh, K.; Inagawa, K.; Kohra, K.; Hayashi, C.; Iida, A. & Kato, N. (1988). Fabrication and Characterization of Multilayer Zone Plate for Hard X-Rays, *Japanese Journal of Applied Physics*, 27, pp. L2131-L2133, ISSN 0021-4922
- Saitoh, K.; Inagawa, K.; Kohra, K.; Hayashi, C.; Iida, A. & Kato, N. (1989). Characterization of sliced multilayer zone plates for hard x rays, *Review of Scientific Instruments*, 60, pp.1519-1523, ISSN 0034-6748
- Schroer, C.G.; Kurapova, O.; Patommel, J.; Boye, P.; Feldkamp, J.; Lengeler, B.; Burgahammer, M.; Riekel, C.; Vincze, L.; Hart, A. van der. & Küchler, M. (2005). Hard x-ray nanoprobe based on refractive x-ray lenses, *Applied Physics Letters*, 87, 124103, ISSN 0003-6951
- Schroer, C.G.; Kurapova, O.; Patommel, J.; Boye, P.; Feldkamp, J.; Lengeler, B.; Burgahammer, M.; Riekel, C.; Vincze, L.; Hart, A. van der. & Küchler, M. (2006). Hard X-Ray Nanoprobe with Refractive X-Ray Lenses, *IPAP Conference Series 7 (Institute of Pure and Applied Physics, Japan)*, pp.94-96, ISBN4-900526-21-5
- Shastri, S.D.; Maser, J.M.; Lai, B. & Tys, J. (2001). Microfocusing of 50 keV undulator radiation with two stacked Zone plates, *Optics Communications*, 197, pp.9-14. ISSN 0030-4018
- Snigirev, A.; Snigireva, I.; Engström, P.; Lequien, S.; Suvorov, A.; Hartman, Ya.; Chevallier, P.; Idir, M.; Legrand, F.; Soullie, G. & Engrand, S. (1995). *Review of Scientific Instruments*, 66, pp.1461-1463, ISSN 0034-6748.
- Snigirev, A.; Kohn, V.; Snigireva, I. & Lengeler, B. (1996): A compound refractive lens for focusing high-energy X-rays, *Nature*, 384, pp.49-51, ISSN 0028-0836

- Snigirev, A.; Snigireva, I.; Michiel, M.Di.; Honkimaki, V.; Grigoriev, M.; Nazmov, V.; Reznikova, E.; Mohr, J. & Saile, V. (2004). Submicron focusing of high-energy x-rays with Ni refractive lenses, *Proc. SPIE (The International Society for Optical Engineering)*, 5539, pp.244-250, ISSN 0277-786X
- Snigirev, A. & Snigireva, I. (2008). Hard X-ray microoptics, *Modern Development in X-ray and Neutron Optics*, p.256, ISBN 978-3-540-74560-0
- Spiller, E. (1994). *Soft X-ray Optics*, P.179, SPIE (The International Society for Optical Engineering) Press, ISBN 0-8184-1654-1
- Suzuki, Y.; Kamijo, N.; Tamura, S.; Handa, K.; Takeuchi, A.; Yamamoto, S.; Sugiyama, H.; Ohsumi, K. & Ando, M. (1997). Hard X-ray Microprobe Experiment at the TRISTAN MAIN Ring Test Beamline of the KEK, *Journal of Synchrotron Radiation*, 4, pp.60-63. ISSN 0909-0495
- Suzuki, Y.; Awaji, M.; Kohmura, Y.; Takeuchi, A.; Takano, H.; Kamijo, N.; Tamura, S.; Yasumoto, M. & Handa, K. (2001). X-ray Microbeam with Sputtered-Sliced Fresnel Zone Plate at SPring-8 Undulator Beamline, *Nuclear Instruments and Methods in Physics Research*, A467-468, pp.951-953, ISSN 0168-9002
- Suzuki, Y.; Takeuchi, A.; Takano, H. & Takenaka, H. (2005). Performance Test of Fresnel Zone Plate with 50nm Outermost Zone Width in Hard X-ray Region, *Japanese Journal of Applied Physics*, 44, pp. 1994-1998, ISSN 0021-4922
- Suzuki, Y.; Takeuchi, A.; Uesugi, K.; Awaji, M.; Yasumoto, M.; Tamura, S. & Kamijo, N. (2006). X-ray Imaging Microscopy at 82 keV with Sputtered-sliced Fresnel Zone Plate Objective, *IPAP Conference Series 7 (Institute of Pure and Applied Physics, Japan)*, pp.47-49, ISBN4-900526-21-5
- Suzuki, Y.; Takeuchi, A.; & Terada, Y. (2007). High-energy x-ray microbeam with total-reflection mirror optics, *Review of Scientific Instruments*, 78,053713, ISSN 0034-6748
- Suzuki, Y. & Takeuchi, A. (2010a). X-ray Microfocusing by Combination of Grazing-Incidence Spherical-Concave Mirrors, *Japanese Journal of Applied Physics*, 49, 106701, ISSN 0021-4922
- Suzuki, Y.; Takeuchi, A.; Takenaka, H. & Okada, I. (2010b). Fabrication and Performance Test of Fresnel Zone Plate with 35nm Outermost Zone Width in Hard X-Ray Region, *X-Ray Optics and Instrumentation (Hindawi Publishing Corporation)*, Article ID 824387, ISSN 1687-7632
- Takeuchi, A.; Uesugi, K., Takano, H. & Suzuki, Y. (2002). Submicrometer-resolution three-dimensional imaging with hard x-ray imaging microtomography, *Review of Scientific Instruments*, 73, pp.4246-4269, ISSN 0034-6748
- Tamura, S.; Ohtani, K. & Kamijo, N. (1994). Materials for Multilayer Zone Plates --- Development of a focusing element for use in SR photo-excited process ---, *Applied Surface Science*, 79/80, 99.514-518, ISSN 0169-4332
- Tamura, S.; Kensuke, M.; Nagao, K.; Yoshida, K.; Kihara, H. & Suzuki, Y. (2000). Focusing efficiency of a multilayer Fresnel zone plate for hard X-ray fabricated by DC sputtering deposition: *Vacuum*, 59, pp.553-558, ISSN 0042-207X
- Tamura, S.; Yasumoto, M.; Mihara, T.; Kamijo, N.; Suzuki, Y.; Awaji, M.; Takeuchi, A.; Takano, H. & Handa, K. (2002). Multilayer Fresnel zone plate for high energy X-rays by DC sputtering deposition: *Vacuum*, 66, pp.495-499, ISSN 0042-207X

- Tamura, S.; Yasumoto, M.; Kamijo, N.; Suzuki, Y.; Awaji, M.; Takauchi, A.; Uesugi, K.; Terada, Y. & Takano, H. (2006). New approaches to fabrication of multilayer Fresnel zone plate for X-rays, *Vacuum*, 80, pp.823-827, ISSN 0042-207X
- Tamura, S.; Yasumoto, M.; Kamijo, N.; Takeuchi, A.; Uesugi, K. & Suzuki, Y. (2008). Multilevel-type multilayer X-ray lens (Fresnel zone plate) by sputter deposition, *Vacuum*, pp.691-694, ISSN 0042-207X
- Tamura, S.; Yasumoto, M.; Kamijo, N.; Takeuchi, A. & Suzuki, Y. (2009). X-ray Focusing Optics with Multilayer Structure and its Application, *Journal of the vacuum society of Japan*, 52, pp.212-217, ISSN 1882-2398
- Takano, H.; Tsuji, T.; Hashimoto, T.; Koyama, T.; Tsusaka, T. & Kagoshima, Y. (2010). Sub-15nm Hard X-Ray Focusing with a New Total-Reflection Zone Plate, *Applied Physics Express*, 3, 076702, ISSN 1882-0778
- Takeuchi, T.; Kageyama, H.; Tamura, S.; Kamijo, N.; Suzuki, Y. & Takeuchi, A. (2005): Preparation of Composite Dielectric Ceramics by Spark-Plasma-Sintering Method, *Proceedings of International Symposium on Novel Materials Processing by Advanced Electromagnetic Energy Source (MAPEES'04)*, pp. 285-288, ISBN 10-0080445047
- Takeuchi, T.; Kageyama, H.; Nakazawa, H.; Atsumi, T.; Tamura, S.; Kamijo, N.; Suzuki, Y. & Takeuchi, A. (2008). Preparation of fluorine-containing indium tin oxide sputtering targets using spark plasma sintering process, *Journal of American Ceramics Society*, 91, pp.2495-2500, ISSN 0002-7820
- Terada, Y.; Suzuki, Y.; Kamijo, N.; Tamura, S.; Onuma, R.; Hokura, A. & Nakai, I. (2004). High Energy Micro-XRF Imaging of Heavy Metals in the Cells of Hyperaccumulator Plants, *Abstract of 8 th International Conference on Biology and Synchrotron Radiation (BSR2004)*
- Terada, Y.; Takeuchi, A.; Suzuki, Y.; Onuma, R.; Shirai, K.; Nakai, I.; Kamijo, N. & Tamura, S. (2005). Development of high energy micro-XRF analysis using fresnel zone plate optics, *Abstract of 8th International Conference of X-ray Microscopy (XRM2005)*, PD22.
- Terada, Y.; Takeda, S.; Homma, S.; Takeuchi, A. and Suzuki, Y. (2010). High-Energy X-Ray Microprobe System with Submicron Resolution for X-Ray Fluorescence Analysis of Uranium in Biological Specimens, *X-Ray Optics and Instrumentation (Hindawi Publishing Corporation)*, Article ID 317909, ISSN 1687-7632
- Thornton, J. A. (1974). Influence of apparatus geometry and deposition conditions on the structure and topography of thick sputtered coatings, *Nuclear Instruments and Methods in Physics Research*, 11, pp.666-670, ISSN 0022-5355
- Thornton, J. A. (1986). The microstructure of sputter-deposited coatings, *Nuclear Instruments and Methods in Physics Research Section J. Vac. Sci. Technol.*, A4, pp.3059-3065, ISSN 0734-2101
- Toda, H.; Uesugi, K.; Takeuchi, A.; Minami, K.; Kobayashi, M. & Kobayashi, T. (2006). Three-dimensional observation of nanoscopic precipitates in an aluminum alloy by microtomography with Fresnel zone plate optics, *Applied Physics Letters*, 89, 143112, ISSN 0003-6951
- Underwood, J.H.; Thompson, A.C.; Wu, Y. & Giauque, R.D. (1988). X-ray microprobe using multilayer mirrors, *Nuclear Instruments and Methods in Physics Research*, A266, pp.296-302, ISSN 0168-9002

- Yasumoto. M.; Tamura, S.; Kamijo, N.; Suzuki, Y.; Awaji, M.; Takeuchi, A.; Takano, H.; Kohmura, Y. & Handa, K. (2001). Suppression of corrugated boundaries in multilayer Fresnel zone plate for synchrotron radiation hard X-ray using cylindrical slit, *Japanese Journal of Applied Physics*, 40, pp.4747-4748, ISSN 0021-4922
- Yun, W. B.; Viccaro, P.J.; Lai, B. & Chrzas. J. (1992). Coherent hard x-ray focusing optics and application, *Review of Scientific Instruments*, 63, pp.582-585, ISSN 0034-6748



Metal, Ceramic and Polymeric Composites for Various Uses

Edited by Dr. John Cuppoletti

ISBN 978-953-307-353-8

Hard cover, 684 pages

Publisher InTech

Published online 20, July, 2011

Published in print edition July, 2011

Composite materials, often shortened to composites, are engineered or naturally occurring materials made from two or more constituent materials with significantly different physical or chemical properties which remain separate and distinct at the macroscopic or microscopic scale within the finished structure. The aim of this book is to provide comprehensive reference and text on composite materials and structures. This book will cover aspects of design, production, manufacturing, exploitation and maintenance of composite materials. The scope of the book covers scientific, technological and practical concepts concerning research, development and realization of composites.

How to reference

In order to correctly reference this scholarly work, feel free to copy and paste the following:

Shigeharu Tamura (2011). Multilayer Fresnel Zone Plate with High-Diffraction Efficiency: Application of Composite Layer to X-Ray Optics, Metal, Ceramic and Polymeric Composites for Various Uses, Dr. John Cuppoletti (Ed.), ISBN: 978-953-307-353-8, InTech, Available from: <http://www.intechopen.com/books/metal-ceramic-and-polymeric-composites-for-various-uses/multilayer-fresnel-zone-plate-with-high-diffraction-efficiency-application-of-composite-layer-to-x-r>

INTech
open science | open minds

InTech Europe

University Campus STeP Ri
Slavka Krautzeka 83/A
51000 Rijeka, Croatia
Phone: +385 (51) 770 447
Fax: +385 (51) 686 166
www.intechopen.com

InTech China

Unit 405, Office Block, Hotel Equatorial Shanghai
No.65, Yan An Road (West), Shanghai, 200040, China
中国上海市延安西路65号上海国际贵都大饭店办公楼405单元
Phone: +86-21-62489820
Fax: +86-21-62489821

© 2011 The Author(s). Licensee IntechOpen. This chapter is distributed under the terms of the [Creative Commons Attribution-NonCommercial-ShareAlike-3.0 License](https://creativecommons.org/licenses/by-nc-sa/3.0/), which permits use, distribution and reproduction for non-commercial purposes, provided the original is properly cited and derivative works building on this content are distributed under the same license.

IntechOpen

IntechOpen